

## **Short- and Medium-term Atmospheric Effects of Very Large Solar Proton Events**

**Charles H. Jackman, Daniel R. Marsh, Francis M. Vitt, Rolando R. Garcia, Eric L. Fleming, Gordon J. Labow, Cora E. Randall, Manuel López-Puertas, and Bernd Funke**

### **Brief, Popular Summary of the Paper:**

Long-term variations in ozone have been caused by both natural and humankind related processes. In particular, the humankind or anthropogenic influence on ozone from chlorofluorocarbons and halons (chlorine and bromine) has led to international regulations greatly limiting the release of these substances. These anthropogenic effects on ozone are most important in polar regions and have been significant since the 1970s. Certain natural ozone influences are also important in polar regions and are caused by the impact of solar charged particles on the atmosphere. Such natural variations have been studied in order to better quantify the human influence on polar ozone.

Large-scale explosions on the Sun near solar maximum lead to emissions of charged particles (mainly protons and electrons), some of which enter the Earth's magnetosphere and rain down on the polar regions. "Solar proton events" have been used to describe these phenomena since the protons associated with these solar events sometimes create a significant atmospheric disturbance.

We have used the National Center for Atmospheric Research (NCAR) Whole Atmosphere Community Climate Model (WACCM) to study the short- and medium-term (days to a few months) influences of solar proton events between 1963 and 2005 on stratospheric ozone. The four largest events in the past 45 years (August 1972; October 1989; July 2000; and October-November 2003) caused very distinctive polar changes in layers of the Earth's atmosphere known as the stratosphere (12-50 km; ~7-30 miles) and mesosphere (50-90 km; 30-55 miles). The solar protons connected with these events created hydrogen- and nitrogen- containing compounds, which led to the polar ozone destruction. The hydrogen-containing compounds have very short lifetimes and lasted for only a few days (typically the duration of the solar proton event). On the other hand, the nitrogen-containing compounds lasted much longer, especially in the Winter. The nitrogen oxides were predicted to increase substantially due to these solar events and led to mid- to upper polar stratospheric ozone decreases of over 20%. These WACCM results generally agreed with satellite measurements. Both WACCM and measurements showed enhancements of nitric acid, dinitrogen pentoxide, and chlorine nitrate, which were indirectly caused by these solar events. Solar proton events were shown to cause a significant change in the polar stratosphere and need to be considered in understanding variations during years of strong solar activity.

# Short- and medium-term atmospheric effects of very large solar proton events

Charles H. Jackman<sup>1</sup>, Daniel R. Marsh<sup>2</sup>, Francis M. Vitt<sup>2</sup>, Rolando R. Garcia<sup>2</sup>, Eric L. Fleming<sup>1</sup>, Gordon J. Labow<sup>1</sup>, Cora E. Randall<sup>3</sup>, Manuel López-Puertas<sup>4</sup>, and Bernd Funke<sup>4</sup>

[1] {NASA/Goddard Space Flight Center, Greenbelt, MD}

[2] {National Center for Atmospheric Research, Boulder, CO}

[3] {University of Colorado, Boulder, CO}

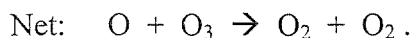
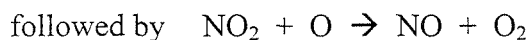
[4] {Instituto de-Astrofísica de Andalucía, CSIC, Granada, SPAIN}

Correspondence to C. H. Jackman (Charles.H.Jackman@nasa.gov)

## Abstract

Solar eruptions sometimes produce protons, which impact the Earth's atmosphere. These solar proton events (SPEs) generally last a few days and produce high energy particles that precipitate into the Earth's atmosphere. The protons cause ionization and dissociation processes that ultimately lead to an enhancement of odd-hydrogen and odd-nitrogen in the polar cap regions ( $>60^\circ$  geomagnetic latitude). We have used the Whole Atmosphere Community Climate Model (WACCM3) to study the atmospheric impact of SPEs over the period 1963-2005. The very largest SPEs were found to be the most important and caused atmospheric effects that lasted several months to years after the events. We present the short- and medium-term (days to a few months) atmospheric influence of the four largest SPEs in the past 45 years (August 1972; October 1989; July 2000; and October-November 2003) as computed by WACCM3 and observed by satellite instruments. The polar effects can be summarized as follows: 1) Mesospheric  $\text{NO}_x$  ( $\text{NO}+\text{NO}_2$ ) increased by over 50 ppbv and mesospheric ozone decreased by over 30% during these very large SPEs; 2) upper stratospheric and lower mesospheric  $\text{NO}_x$  increased by over 10 ppbv and was transported during polar night down to the middle stratosphere in a few weeks; 3) mid- to upper stratospheric ozone decreased over 20%; and 4) enhancements of  $\text{HNO}_3$ ,  $\text{HOCl}$ ,  $\text{ClO}$ ,  $\text{ClONO}_2$ , and  $\text{N}_2\text{O}_5$  were indirectly caused by the very large SPEs, although the

The SPE-produced  $\text{NO}_x$  constituents lead to short- and longer-term catalytic ozone destruction in the lower mesosphere and stratosphere (pressures greater than about 0.5 hPa) via the well-known  $\text{NO}_x$ -ozone loss cycle



There have been a number of modeling studies focused on understanding and predicting the atmospheric influence of SPEs [e.g., Warneck, 1972; Swider and Keneshea, 1973; Crutzen et al., 1975; Swider et al., 1978; Banks, 1979; Fabian et al., 1979; Jackman et al., 1980, 1990, 1993, 1995, 2000, 2007; Solomon and Crutzen, 1981; Rusch et al., 1981; Solomon et al., 1981, 1983; Reagan et al., 1981; Jackman and McPeters, 1985; Roble et al., 1987; Reid et al., 1991; Vitt and Jackman, 1996; Vitt et al., 2000; Krivolutsky et al., 2001, 2003, 2005, 2006; Verronen et al., 2002, 2005, 2006; Semeniuk et al., 2005]. Most of these studies were carried out with lower dimensional models (0-D, 1-D, 2-D); however, a few used three-dimensional (3-D) models [e.g., Jackman et al., 1993, 1995, 2007; Semeniuk et al., 2005; Krivolutsky et al., 2006] to investigate the more detailed global effects of SPEs.

In this study we have used version 3 of the Whole Atmosphere Community Climate Model (WACCM3), which is a general circulation model with complete interactive photochemistry with a domain that extends from the ground to the lower thermosphere. The recent development of WACCM3 allows study of the detailed time-dependent 3-D atmospheric response to a variety of perturbations. The purpose of this work is to use WACCM3 to investigate the global effects of SPEs over solar cycles 20-23 (years 1963-2005). The short- and medium-term (days to months) atmospheric influence will be shown with particular attention to the SPE-induced changes in stratospheric and mesospheric (middle atmospheric) composition. We have observations from several satellite instruments documenting SPE effects during the most recent solar maximum period (solar cycle 23, years 2000-2005) to help verify WACCM3 predictions. We also have a few satellite instrument measurements of atmospheric impacts during the very large SPEs of August 1972 and October 1989 with which to compare.

This paper is divided into seven primary sections, including the Introduction. The solar proton flux and ionization rate computation are discussed in Section 2 and SPE-induced production of  $\text{HO}_x$  and  $\text{NO}_y$  are discussed in Section 3. A description of the satellite instrument measurements and WACCM3

The daily average ion pair production rates for years 1963-2005 were computed from the energy deposition assuming 35 eV/ion-pair. An example of the daily average ionization rate ( $\text{cm}^{-3}\text{s}^{-1}$ ) is given in Figure 1 for a thirteen day period in October- November 2003, a very intense period of SPEs. The October 28-31, 2003 SPE period was the fourth largest of the past 45 years (see Table 1). Very large daily average ionization rates of  $>5000 \text{ cm}^{-3}\text{s}^{-1}$  extending from 0.01 to 1. hPa are computed for Oct. 29, 2003. Large ionization rates  $>1000 \text{ cm}^{-3}\text{s}^{-1}$  extending from the upper stratosphere through the mesosphere are computed for Oct. 28-30, 2003.

These ionization rate data are provided as functions of pressure between 888 hPa ( $\sim 1 \text{ km}$ ) and  $8 \times 10^{-5}$  hPa ( $\sim 115 \text{ km}$ ) at the SOLARIS (Solar Influence for SPARC) website (<http://strat-www.met.fu-berlin.de/~matthes/sparc/inputdata.html>) and can be used in model simulations.

### 3 Odd Hydrogen ( $\text{HO}_x$ ) and Odd Nitrogen ( $\text{NO}_y$ ) Production

#### 3.1 Odd Hydrogen ( $\text{HO}_x$ ) Production

Protons and their associated secondary electrons also produce odd hydrogen ( $\text{HO}_x$ ). The production of  $\text{HO}_x$  takes place after the initial formation of ion-pairs and is the end result of complex ion chemistry [Swider and Keneshea, 1973; Frederick, 1976; Solomon et al. 1981]. Generally, each ion pair results in the production of approximately two  $\text{HO}_x$  species in the upper stratosphere and lower mesosphere. In the middle and upper mesosphere, an ion pair is calculated to produce less than two  $\text{HO}_x$  species. The  $\text{HO}_x$  production from SPEs is included in WACCM3 using a lookup table from Jackman et al. [2005a, Table 1], which is based on the work of Solomon et al. [1981]. The  $\text{HO}_x$  constituents are quite reactive with each other and have a relatively short lifetime ( $\sim$ hours) throughout most of the mesosphere [Brasseur and Solomon, 1984, see Figure 5.28] and thus are important only during and shortly after solar events.

#### 3.2 Odd Nitrogen ( $\text{NO}_y$ ) Production

Odd nitrogen is produced when the energetic charged particles (protons and associated secondary electrons) collide with and dissociate  $\text{N}_2$ . We assume that  $\sim 1.25 \text{ N}$  atoms are produced per ion pair and divide the proton impact of N atom production between ground state ( $\sim 45\%$  or  $\sim 0.55$  per ion pair) and excited state ( $\sim 55\%$  or  $\sim 0.7$  per ion pair) nitrogen atoms [Porter et al., 1976]. Following the discussion

chemistry of the Earth's atmosphere. This model has been developed over the past seven years and has become a useful tool for investigating the coupling among the various atmospheric regions from the troposphere through the middle atmosphere to the lower thermosphere [Sassi et al., 2002, 2004; Forkman et al., 2003; Richter and Garcia, 2006; Garcia et al., 2007].

## **4.2 WACCM3 Simulations**

WACCM3 was forced with observed time-dependent sea surface temperatures (SSTs), observed solar spectral irradiance and geomagnetic activity changes, and observed concentrations of greenhouse gases and halogen species over the simulation periods [see Garcia et al., 2007]. We have completed a number of WACCM3 simulations, some with the daily ionization rates from SPEs and some without. The ionization rates, when included, were applied uniformly over both polar cap regions (60-90°N and 60-90°S geomagnetic latitude) as solar protons are guided by the Earth's magnetic field lines to these areas [McPeters et al., 1981; Jackman et al., 2001, 2005a]. The effects are not expected to be symmetric between the hemispheres because of the differing offsets of geomagnetic and geographic poles. A list of the WACCM3 simulations and their designation in this study is given in Table 2.

Since the year 1989 was very active in terms of SPEs (see Table 1), simulations with SPEs [see 2(a,b,c,d)] and without SPEs [see 2(w,x,y,z)] were performed to study the 15 month period, Jan. 1, 1989 – Mar. 31, 1990. The very large July 2000 SPE was studied in further detail over the period July 2 – September 30, 2000 using simulations with SPEs [see 3(a,b,c,d)] and without SPEs [see 3(w,x,y,z)]. The very large late October/early November 2003 SPEs were studied in further detail over the period October 25 – November 14, 2003 using a simulation with SPEs [see 4(a)] and without SPEs [see 4(w)]. Simulations 1(a,b,c,d), 2(a,b,c,d), and 2(w,x,y,z) have model output every five days. Simulations 3(a,b,c,d), 3(w,x,y,z), 4(a), and 4(w) have model output every day. For short periods (~two weeks), different realizations produce similar results; thus it is appropriate to use only a single realization for simulation 4.

## **4.3 Satellite Instrument Measurements**

Several satellite instruments have recorded atmospheric constituent change caused by SPEs. We will compare WACCM3 results with:

- 1) Nimbus 4 Backscatter Ultraviolet (BUV) ozone measurements (August 1972 SPEs);

Space Agency (CSA) Atmospheric Chemistry Experiment (ACE), and MIPAS in the Northern Hemisphere in February-April 2004 were possibly caused by the downward transport of this thermospheric NO<sub>x</sub> to lower atmospheric levels [Natarajan et al. 2004, Rinsland et al. 2005, and Randall et al. 2005].

## 5.1 HO<sub>x</sub> (H, OH, HO<sub>2</sub>) Constituents

The ‘Halloween Storms’ of 2003 caused SPEs, which produced HO<sub>x</sub> constituents. The HO<sub>x</sub> changes simulated by WACCM3 are presented in Figure 3 for the southern (70-90°S; left) and northern (70-90°N; right) polar regions from simulation 4(a). Huge HO<sub>x</sub> increases are predicted during the most intense periods of the SPEs reaching over 100% and 700% near 0.1 hPa in the southern and northern polar regions, respectively. Since the HO<sub>x</sub> species have a relatively short lifetime (hours), these very short-term effects disappear almost entirely by the end of November 6. HO<sub>x</sub> changes after this date are due to the normal seasonal behavior in those regions as sunlight increases (decreases) in the southern (northern) polar regions at this time of year, leading to increases (decreases) in HO<sub>x</sub> as the sources of HO<sub>x</sub> [ $\text{H}_2\text{O} + \text{O}(^1\text{D}) \rightarrow 2\text{OH}$  and  $\text{H}_2\text{O} + h\nu \rightarrow \text{H} + \text{OH}$ ] are affected. The enhanced HO<sub>x</sub> constituents produced by the SPEs led to short-term ozone destruction, especially in the mesosphere and upper stratosphere.

## 5.2 NO<sub>x</sub> (N, NO, NO<sub>2</sub>) Constituents

The NO<sub>x</sub> species have considerably longer lifetimes than the HO<sub>x</sub> species and are produced in great abundance during very large SPEs. For example, we have evidence of huge enhancements of NO<sub>x</sub> as a result of the ‘Halloween Storms’ of 2003. The Envisat MIPAS instrument provided simultaneous observations of NO<sub>x</sub> in both polar regions. Atomic nitrogen (N) is quite small in the mesosphere and stratosphere; thus, the MIPAS measurements of NO and NO<sub>2</sub> essentially provide a measure of the polar NO<sub>x</sub> enhancements during the ‘Halloween Storms’ of 2003. We show the MIPAS Northern Hemisphere polar NO<sub>x</sub> on three days (Oct. 27, 29, and 30) in Figure 4 (top) at the 2250 K (50-55 km) surface. The polar vortex edge has been calculated using the Nash criterion [Nash et al., 1996] but modified so that a dynamical tracer (CH<sub>4</sub> below 1500 K and CO above) has been used, instead of the mean zonal winds. This vortex boundary is represented with a red curve and the geomagnetic pole is marked with a red plus sign. Some individual NO<sub>x</sub> values reached 180 ppbv, about a factor of ten

same regions in Figure 6 (bottom). Due to the short lifetime of  $\text{HO}_x$  constituents (see Figure 3), their ozone influence lasts only during and for a few hours after the SPEs. This explains the huge measured and modeled ozone depletion on Oct. 29-30 and, to a lesser extent, on Nov. 3-4. Note that Figure 1 shows ion pair production, which is essentially a proxy for the  $\text{NO}_x$  and  $\text{HO}_x$  production.

SPE impacts in the NH are larger than the SH in both models and simulations. NH ozone depletion exceeds 50% during the SPEs in late October. Polar NH upper stratospheric ozone depletion greater than 30% continues through Nov. 14, the end of the plotting period. The polar SH shows ozone reduction greater than 30% during the SPEs in late October with lower mesospheric ozone depletion from 5-10% continuing through Nov. 14.

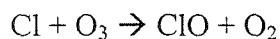
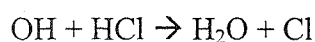
The measured and modeled ozone depletions do show some differences. The NH modeled ozone indicates a larger recovery (ozone enhancement) above  $\sim 57$  km after Nov. 7, than indicated in the measurements. This apparent NH ozone recovery is due to seasonal changes, wherein ozone is enhanced via transport from above. The SH modeled ozone below  $\sim 45$  km indicates a larger ozone depletion after Nov. 2, than indicated in the measurements. The reason(s) behind these NH and SH model-measurement differences are still unclear, but is probably caused in part by the fact that transport in WACCM is not meant to simulate any specific year.

Other measurements of short-term ozone loss caused by solar protons are available for other SPEs. For example, a very large SPE commenced on July 14, 2000, the so-called ‘Bastille Day’ solar storm, which was the third largest SPE period in the past 45 years. This SPE took place over the July 14-16 period. Jackman et al. [2001] showed Northern Hemisphere polar ozone changes (in ppmv) from the NOAA 14 SBUV/2 instrument at 0.5 hPa due to the July 2000 SPE between July 13 (before SPE) and July 14-15 (during SPE), 2000. We provide a similar plot in Figure 7, which shows the percentage change for ozone from July 13 to July 14-15 for NOAA 14 SBUV/2 and from July 13 to July 15 at 0:00 GMT from WACCM3 simulation 3(a). Figure 7 (left) is constructed from 24 hours of NOAA 14 SBUV/2 orbital data during the maximum intensity of the event and Figure 7 (right) is a difference of model “snapshots.”

The polar cap edge ( $60^\circ$  geomagnetic latitude), wherein the protons are predicted to interact with the atmosphere, is indicated by the white circle. Large ozone decreases of 30-40% are seen at this pressure level in both the SBUV/2 observations and WACCM3 calculations, which are primarily caused by the SPE. These ozone decreases are driven by catalytic destruction from the  $\text{HO}_x$  increases of  $\sim 100\%$  and

nighttime in the polar Northern Hemisphere (70-90°N) is taken from Figure 5 of Lopez-Puertas et al. [2005b] and shown in Figure 9 (top). The N<sub>2</sub>O<sub>5</sub> modeled [simulation 4(a)] enhancements peaked between 30 and 50 km near the last day plotted (Nov. 14), similar to the MIPAS observations. WACCM3 predicted N<sub>2</sub>O<sub>5</sub> increases of 5-6 ppbv (primarily driven by the SPEs) were, however, significantly larger than the MIPAS measured increases of about 1 ppbv. WACCM3 predicted seasonal changes in N<sub>2</sub>O<sub>5</sub> are shown in Figure 9 (bottom) from a computation **without** SPEs [simulation 4(w)]. This plot indicates the importance of the seasonal changes in forcing the N<sub>2</sub>O<sub>5</sub> enhancement of 0.6 ppbv between 25 and 35 km from October 26-31, 2003. The seasonal changes contribute only modestly to the N<sub>2</sub>O<sub>5</sub> increases in the mid- to upper stratosphere (30-50 km) in November 2003, so the cause of the discrepancy between the model and measurements at these altitudes is not understood..

Envisat MIPAS measurements and WACCM3 computations of HOCl simulation 4(a) are presented for the polar Northern Hemisphere (70-90°N) in the top and bottom of Figure 10, respectively. Both model and measurement show very significant HOCl enhancements in the altitude range 35-55 km. The mechanism for increasing HOCl as a result of the SPEs involves enhancing the HO<sub>x</sub> constituents, which then speed up the following gas-phase three reaction sequence:



Generally, the measurements and model predictions are in agreement, although there is a slight disagreement in the altitude range of the effect. The measurements indicate HOCl increases all the way down to 30 km, whereas WACCM3 calculates HOCl increases from 35 km up to 60 km and above. Both measurements and model show a HOCl peak on Oct. 29; however, the WACCM3 peak is about 0.1-0.15 ppbv larger. WACCM3 results also show a secondary HOCl peak on Nov. 4 due to a smaller SPE in this period (Figure 1). We also investigated model predictions in the WACCM3 computation **without** SPEs [simulation 4(w)] and found very small changes over this period, implying that most of the measured and modeled HOCl changes were due to the SPEs.

Our simulations also provided information on ClO and ClONO<sub>2</sub> changes during and shortly after the SPEs during the ‘Halloween Storms’ of 2003, which are not shown in this study. WACCM3 ClO enhancements peaked near 0.3 ppbv on Oct. 29, similar to the MIPAS observations [von Clarmann et al., 2005]. However, the model enhancements were largest above 50 km and the MIPAS increases



responsible for the short-lived large ozone decreases ( $>40\%$ ). The SPE-caused enhanced  $\text{NO}_x$  then drives the ozone depletion after this period. By about day 255 (September 11), a  $\text{NO}_x$  increase of  $>5$  ppbv appears to cause an ozone loss of  $>10\%$ . The rate of descent of the  $\text{NO}_x$  and ozone perturbation is about 140 m/day ( $\sim 0.16$  cm/s) over this period.

Is there any evidence of SPE-caused  $\text{NO}_x$  enhancements lasting at least six weeks after the event period, as simulated by WACCM3? Yes: Randall et al. [2001] showed evidence from HALOE observations of large  $\text{NO}_x$  ( $\text{NO} + \text{NO}_2$ ) enhancements two months after this July 2000 SPE in the Southern Hemisphere. The  $\text{NO}_x$  increases in September 2000 in the polar vortex were almost certainly caused by the July 2000 SPE (see Figure 12, left). Ten years of HALOE observations are presented in Figure 12 (left). Although there is evidence of interannual variability, the year 2000 shows enhancements of  $\text{NO}_x$  by about a factor of 2-3 beyond the normal range near 1000K ( $\sim 33$  km).

We have sampled the WACCM3 output of simulation 1(a) in a similar manner and present the results in Figure 12 (right side). The WACCM3 results indicate somewhat larger interannual variability above about 32 km, and less variability below this altitude. However, year 2000 shows a clear enhancement beyond the normal range that is analogous to the HALOE measurements. The sharper peak in WACCM3 is likely related to the coarser altitude grid in the model. There are differences in the interannual variability in WACCM3 compared with HALOE near the top level shown (1500 K,  $\sim 40$  km) in Figure 12. It is unclear what the differences in variability mean, although a strong possibility is different dynamics in the model and actual atmosphere. For instance, the local maxima near 700-800 K in the HALOE data likely result from downward transport of  $\text{NO}_x$  produced earlier in the winter at higher altitudes by energetic particle precipitation [see Randall et al., 2007]; WACCM3 might not be simulating this transport adequately. Recall that since the version of WACCM3 used here is not forced by analyzed winds, we do not expect the model dynamics to match the atmospheric dynamics in detail for any specific year.

## 6.2 August 1972 Solar Proton Events

The second largest SPE period in the past 45 years occurred August 2-10, 1972 (days 215-223).. Although this SPE period occurred about 35 years ago, there were recorded measurements of its ozone impact [e.g., Heath et al., 1977; Reagan et al., 1981; McPeters et al., 1981; Jackman and McPeters, 1987; Jackman et al., 1990]. We compare our WACCM3 predicted ozone changes to measured ozone changes from the backscattered ultraviolet (BUV) instrument on the Nimbus 4 satellite between about

12% for the NH. Although there are quantitative differences between WACCM3 and SBUV/2 measurements, the prediction of a substantially larger ozone depletion in the NH than the SH in December 1989 is similar to the measurements. These WACCM3 results complement the three-dimensional chemistry-transport-model results given in Jackman et al. [1995].

SAGE II ozone and NO<sub>2</sub> measurements over five months after this extreme proton flux period have been reported before in a comparison with 3D model predictions [Jackman et al., 1995]. SAGE II observations and WACCM3 simulation results are presented for NO<sub>2</sub> (Figure 15, top) and ozone (Figure 15, bottom) for March 31, 1990. The SAGE II observations were derived by computing the percentage difference on March 31, 1990 compared with March 31, 1987 and are represented by the solid line with asterisks. WACCM3 (case 1) results, represented by the dotted line, were derived using the ensemble mean of simulations 1(a,b,c,d) and computing the percentage difference on March 31, 1990 compared with March 31, 1987. WACCM3 (case 2) results, represented by the dashed line, was derived from the ensemble average of simulations 2(a,b,c,d) differenced with the ensemble average of simulations 2(w,x,y,z) for March 31, 1990.

SAGE II measurements and WACCM3 predictions show large enhancements in NO<sub>2</sub> on March 31, 1990 (Figure 15, top): ~68% at 21 km for SAGE II; ~105% at 22 km for WACCM3 (case 1); and ~34% at 22 km for WACCM3 (case 2). These results point to a substantial downward transport of NO<sub>y</sub> (in general) and NO<sub>2</sub> (in particular) after the SPEs (also, see Figure 14, top). Although there are differences between the model simulations and measurements in the absolute amount of enhanced NO<sub>2</sub> on March 31, 1990 as a result of the October 1989 SPEs, it is clear that these SPEs have led to an increase in NO<sub>2</sub>. Some of the differences between WACCM3 and SAGE II NO<sub>2</sub> changes are probably related to interannual variability [see discussion in Jackman et al., 1995]. Randall et al. [2006] also showed that varying meteorology plays a substantial role in determining the distribution of NO<sub>x</sub> in the NH middle atmosphere several months after energetic particle precipitation. Differences in medium-term changes in composition between the model and measurements are thus expected for these climatological WACCM3 runs.

The measured and modeled decreases in ozone are in qualitative agreement near 25 km (Figure 15, bottom): ~11% for SAGE II; ~10% for WACCM3 (case 1); and ~5% for WACCM3 (case 2). The measured and modeled ozone changes above 25 km indicate substantial variations with altitude. The polar regions have large interannual dynamical variations in both measurements and model simulations; thus, it is difficult to predict precisely the ozone impact over five months after this extremely large SPE period.

## References

- Armstrong, T. P., C. Brundardt, and J. E. Meyer, Satellite observations of interplanetary and polar cap solar particle fluxes from 1963 to the present, in *Weather and Climate Response to Solar Variations*, edited by B. M. McCormac, pp. 71-79, Colorado Associated University Press, Boulder, 1983.
- Banks, P. M., Joule heating in the high-latitude mesosphere, *J. Geophys. Res.*, **84**, 6709-6712, 1979.
- Brasseur, G., and S. Solomon, *Aeronomy of the Middle Atmosphere*, D. Reidel Publishing Company, Dordrecht, Holland, 1984.
- Crutzen, P. J., I. S. A. Isaksen, and G. C. Reid, Solar proton events: Stratospheric sources of nitric oxide, *Science*, **189**, 457-458, 1975.
- Fabian, P., J. A. Pyle, and R. J. Wells, The August 1972 solar proton event and the atmospheric ozone layer, *Nature*, **277**, 458-460, 1979.
- Forkman, P., P. Eriksson, A. Winnberg, R. R. Garcia, and D. Kinnison, Longest continuous ground-based measurements of mesospheric CO, *Geophys. Res. Lett.*, **30**, 1532, doi:10.1029/2003GL016931, 2003.
- Frederick, J. E., Solar corpuscular emission and neutral chemistry in the Earth's middle atmosphere, *J. Geophys. Res.*, **81**, 3179-3186, 1976.
- Garcia, R. R., D. Marsh, D. Kinnison, B. Boville, and F. Sassi, Simulation of secular trends in the middle atmosphere, *J. Geophys. Res.*, **111**, doi:10.1029/2006JD007485, in press, 2007.
- Heath, D. F., A. J. Krueger, and P. J. Crutzen, Solar proton event: influence on stratospheric ozone, *Science*, **197**, 886-889, 1977.
- Jackman, C. H., and R. D. McPeters, The response of ozone to solar proton events during solar cycle 21: A theoretical interpretation, *J. Geophys. Res.*, **90**, 7955-7966, 1985.
- Jackman, C. H., and R. D. McPeters, Solar proton events as tests for the fidelity of middle atmosphere models, *Physica Scripta*, **T18**, 309-316, 1987.
- Jackman, C. H., and R. D. McPeters, The Effect of Solar Proton Events on Ozone and Other Constituents," in *Solar Variability and its Effects on Climate*, *Geophys. Mon.* **141**, 305-319, 2004.
- Jackman, C. H., J. E. Frederick, and R. S. Stolarski, Production of odd nitrogen in the stratosphere and mesosphere: An intercomparison of source strengths, *J. Geophys. Res.*, **85**, 7495-7505, 1980.

Krivolutsky, A., A. Ondraskova, and J. Lastovicka, Photochemical response of neutral and ionized middle atmosphere composition to the strong solar proton event of October 1989, *Adv. Sp. Res.*, 27, 1975-1981, 2001.

Krivolutsky, A., A. Kuminov, T. Vyushkova, N. Pereyaslova, and M. Nazarova, Proton activity of the Sun during 23<sup>rd</sup> solar maximum and its response in ozonosphere of the Earth, *Adv. Sp. Res.*, 31, 2151-2156, 2003.

Krivolutsky, A., A. Kuminov, and T. Vyushkova, Ionization of the atmosphere caused by solar protons and its influence on ozonosphere of the Earth during 1994-2003, *J. Atmos. Solar-Terr. Phys.*, 67, 105-117, 2005.

Krivolutsky, A. A., A. V. Klyuchnikova, G. R. Zakharov, T. Yu. Byushkova, and A. A. Kuminov, Dynamical response of the middle atmosphere to solar proton event of July 2000: Three-dimensional model simulations, *Adv. Sp. Res.*, 37, 1602-1613, 2006.

López-Puertas, M., B. Funke, S. Gil-López, T. von Clarmann, G.P. Stiller, M. Höpfner, S. Kellmann, H. Fischer, and C.H. Jackman, Observation of NO<sub>x</sub> enhancement and ozone depletion in the Northern and Southern Hemispheres after the October-November 2003 solar proton events, *J. Geophys. Res.*, 110, A09S43, doi:10.1029/2005JA011050, 2005a.

López-Puertas, M., B. Funke, S. Gil-López, G. Mengistu Tsidu, H. Fischer, and C. H. Jackman, HNO<sub>3</sub>, N<sub>2</sub>O<sub>5</sub>, and ClONO<sub>2</sub> enhancements after the October-November 2003 solar proton events, *J. Geophys. Res.*, 110, A09S44, doi:10.1029/2005JA011051, 2005b.

McPeters, R. D., A nitric oxide increase observed following the July 1982 solar proton event, *Geophys. Res. Lett.*, 13, 667-670, 1986.

McPeters, R. D., and C. H. Jackman, The response of ozone to solar proton events during solar cycle 21: the observations, *J. Geophys. Res.*, 90, 7945-7954, 1985.

McPeters, R. D., C. H. Jackman, and E. G. Stassinopoulos, Observations of ozone depletion associated with solar proton events, *J. Geophys. Res.*, 86, 12,071-12,081, 1981.

Nash, E. R., P. A. Newman, J. E. Rosenfield, and M. R. Schoeberl, An objective determination of the polar vortex using Ertel's potential vorticity, *J. Geophys. Res.*, 101, 9471-9478, 1996.

Natarajan, M., E. E. Remsberg, L. E. Deaver, and J. M. Russell III, Anomalous high levels of NO<sub>x</sub> in the polar upper stratosphere during April, 2004: Photochemical consistency of HALOE observations, *Geophys. Res. Lett.*, 31, L15113, doi:10.1029/2004GL020566, 2004.

heating in the mesosphere and thermosphere during the July 13, 1982, solar proton event, *J. Geophys. Res.*, **92**, 6083-6090, 1987.

Rohen, G., C. von Savigny, M. Sinnhuber, E. J. Llewellyn, J. W. Kaiser, C. H. Jackman, M. -B. Kallenrode, J. Schroter, K. -U. Eichmann, H. Bovensmann, and J. P. Burrows, Ozone depletion during the solar proton events of Oct./Nov. 2003 as seen by SCIAMACHY, *J. Geophys. Res.*, **110**, A09S39, doi:10.1029/2004JA010984, 2005.

Rusch, D. W., J.-C. Gerard, S. Solomon, P. J. Crutzen, and G. C. Reid, The effect of particle precipitation events on the neutral and ion chemistry of the middle atmosphere, 1, Odd nitrogen, *Planet. Space Sci.*, **29**, 767-774, 1981.

Sassi, F., R. R. Garcia, B. A. Boville, and H. Liu, On temperature inversions and the mesospheric surf zone, *J. Geophys. Res.*, **107**, 4380, doi:10.1029/2001JD001525, 2002.

Sassi, F., D. Kinnison, B. A. Boville, R. R. Garcia, and R. Roble, Effect of El Nino-Southern Oscillation on the dynamical, thermal, and chemical structure of the middle atmosphere, *J. Geophys. Res.*, **109**, D17108, doi:10.1029/2003JD004434, 2004.

Semeniuk, K., J. C. McConnell, and C. H. Jackman, Simulation of the October-November 2003 solar proton events in the CMAM GCM: Comparison with observations, *Geophys. Res. Lett.* **32**, L15S02, doi:10.1029/2004GL022392, 2005.

Seppälä, A., P.T. Verronen, E. Kyrölä, S. Hassinen, L. Backman, A. Hauchecorne, J.L. Bertaux, and D. Fussen, Solar proton events of October-November 2003: Ozone depletion in the Northern Hemisphere polar winter as seen by GOMOS/Envisat, *Geophys. Res. Lett.*, **31**, L19107, doi:10.1029/2004GL021042, 2004.

Seppälä, A., P.T. Verronen, V.F. Sofieva, J. Tamminen, E. Kyrölä, C. J. Rodger, and M. A. Clilverd, Destruction of the tertiary ozone maximum during a solar proton event, *Geophys. Res. Lett.*, **33**, L07804, doi:10.1029/2005GL025571, 2006.

Solomon, S., and P. J. Crutzen, Analysis of the August 1972 solar proton event including chlorine chemistry, *J. Geophys. Res.*, **86**, 1140-1146, 1981.

Solomon, S., D. W. Rusch, J.-C. Gerard, G. C. Reid, and P. J. Crutzen, The effect of particle precipitation events on the neutral and ion chemistry of the middle atmosphere, 2, Odd hydrogen, *Planet. Space Sci.*, **29**, 885-892, 1981.

Weeks, L. H., R. S. CuiKay, and J. R. Corbin, Ozone measurements in the mesosphere during the solar proton event of 2 November 1969, *J. Atmos. Sci.*, 29, 1138-1142, 1972.

Zadorozhny, A. M., G. A. Tuchkov, V. N. Kikhtenko, J. Lastovicka, J. Boska, and A. Novak, Nitric oxide and lower ionosphere quantities during solar particle events of October 1989 after rocket and ground-based measurements, *J. Atmos. Terr. Phys.*, 54, 183-192, 1992.

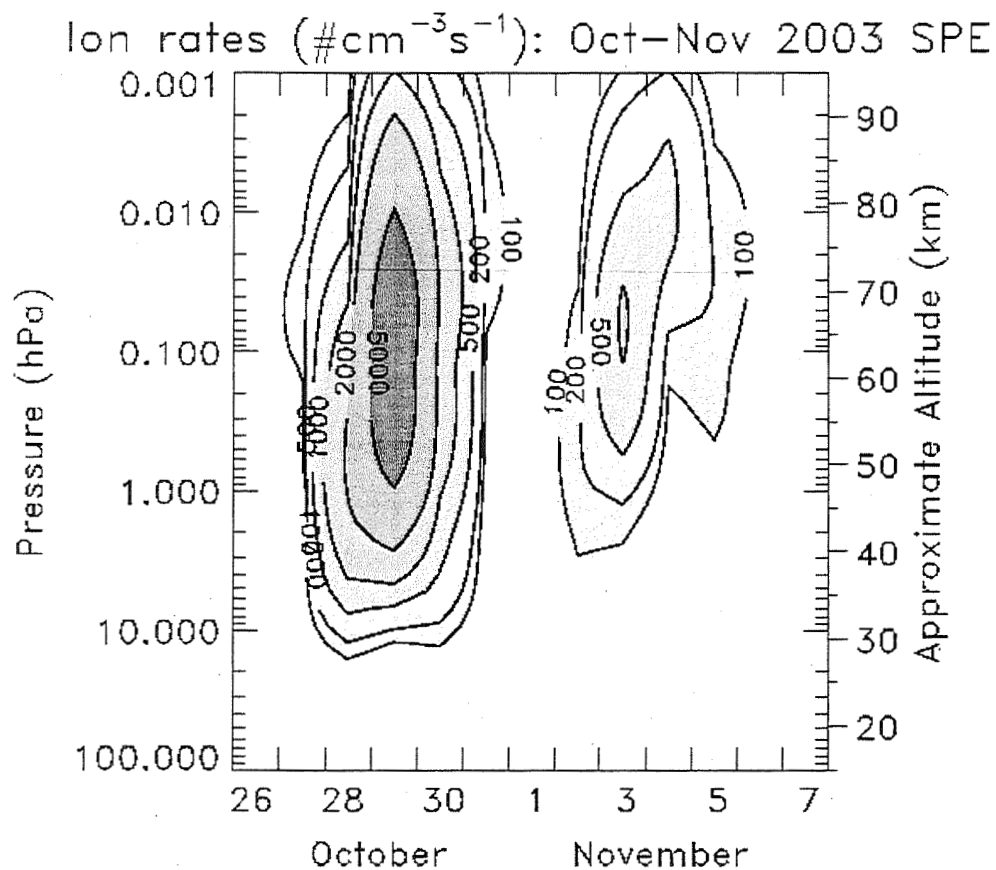


Figure 1. Daily average ion pair production rates using the GOES 11 proton flux measurements for October 26 through November 7, 2003. Contour levels are 100, 200, 500, 1000, 2000, and 5000  $\text{cm}^{-3}\text{s}^{-1}$ .

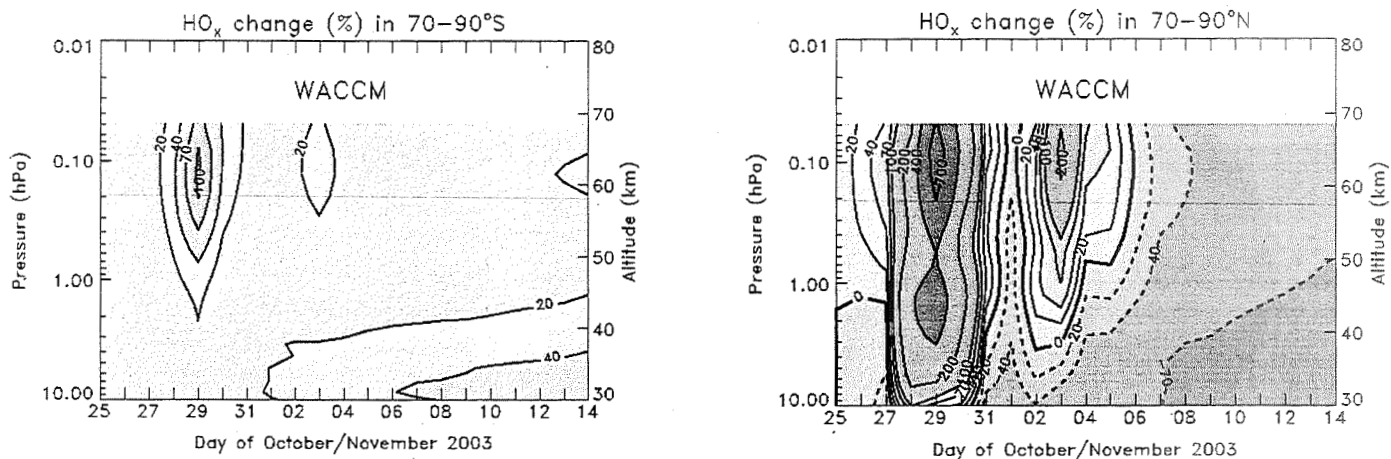


Figure 3. Temporal evolution of  $\text{HO}_x$  (H, OH,  $\text{HO}_2$ ) abundance changes relative to October 25 during and after the October-November 2003 SPEs for the Southern Hemisphere (70-90°S) (left) and Northern Hemisphere (70-90°N) (right) polar caps predicted by WACCM simulation 4(a). Contour levels plotted are -70, -40, -20, 0, 20, 40, 70, 100, 200, 400, and 700%.



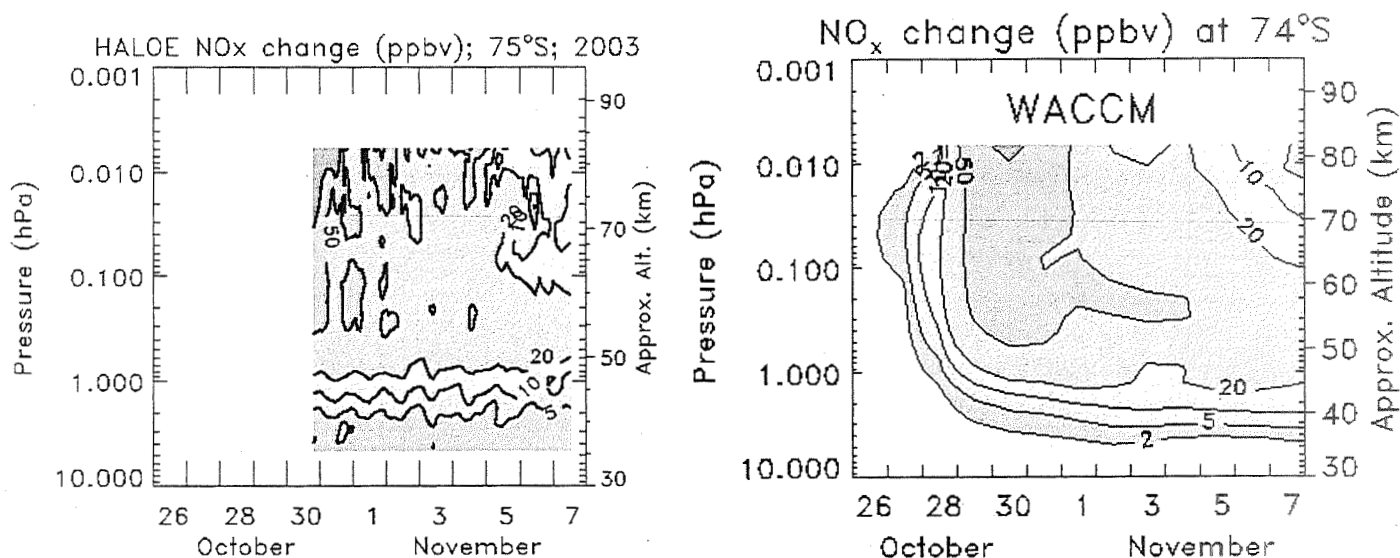


Figure 5. Left plot is taken from Figure 7 of Jackman et al. [2005a] and shows the polar Southern Hemisphere  $\text{NO}_x$  change caused by the late Oct. – early Nov. 2003 SPEs beyond the ambient atmosphere amounts measured Oct. 12-15, 2003. Right plot is derived from WACCM3 simulation 4(a) and indicates the  $\text{NO}_x$  change caused by the Oct.-Nov. 2003 SPEs beyond the ambient atmosphere amounts on Oct. 25 (before the SPEs). Contour levels plotted are 2, 5, 10, 20, 50, and 100 ppbv.

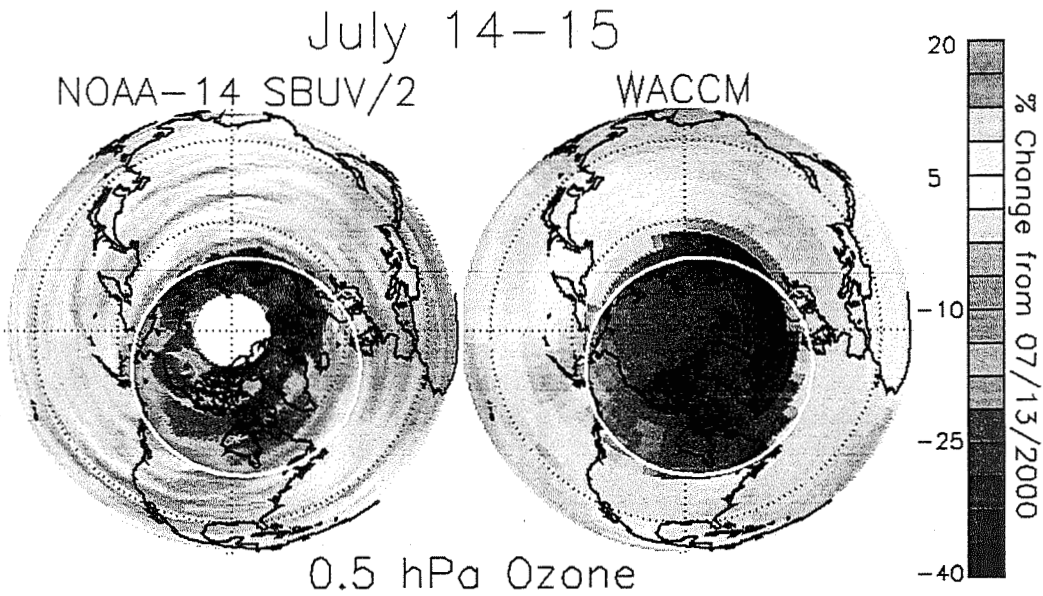


Figure 7. Left plot shows NOAA-14 SBUV/2 Northern Hemisphere polar ozone percentage change at 0.5 hPa from July 13, 2000 (before the SPE) to July 14-15, 2000 (maximum proton intensity). Right plot shows WACCM3 ‘snapshot’ using simulation 3(a) of polar ozone percentage change at 0.5 hPa for 0:00 GMT from July 13 to July 15, 2000.

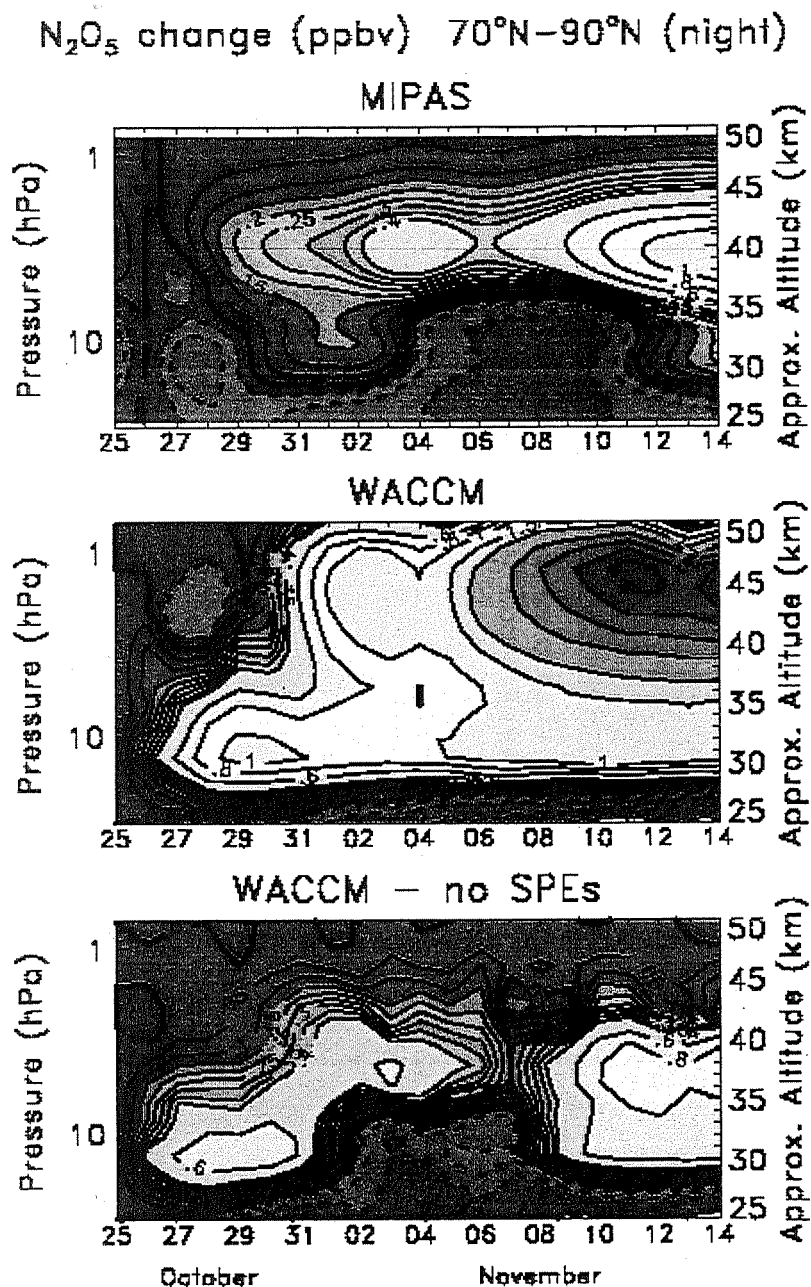


Figure 9. Top plot is taken from Figure 5 of Lopez-Puertas [2005b] and shows the temporal evolution of MIPAS  $\text{N}_2\text{O}_5$  abundance changes relative to October 26 for nighttime in the polar Northern Hemisphere (70–90°N). Middle plot is derived from WACCM3 simulation 4(a) and indicates  $\text{N}_2\text{O}_5$  changes relative to October 25 for night in 70–90°N. Bottom plot is derived from WACCM3 simulation 4(w) indicates  $\text{N}_2\text{O}_5$  changes relative to October 25 for night in 70–90°N. Contour levels plotted are -0.6, -0.4, -0.2, -0.1, -0.05, 0.0, 0.05, 0.1, 0.15, 0.2, 0.25, 0.3, 0.35, 0.4, 0.6, 0.8, 1.0, 1.5, 2, 3, 4, 5, and 6 ppbv.

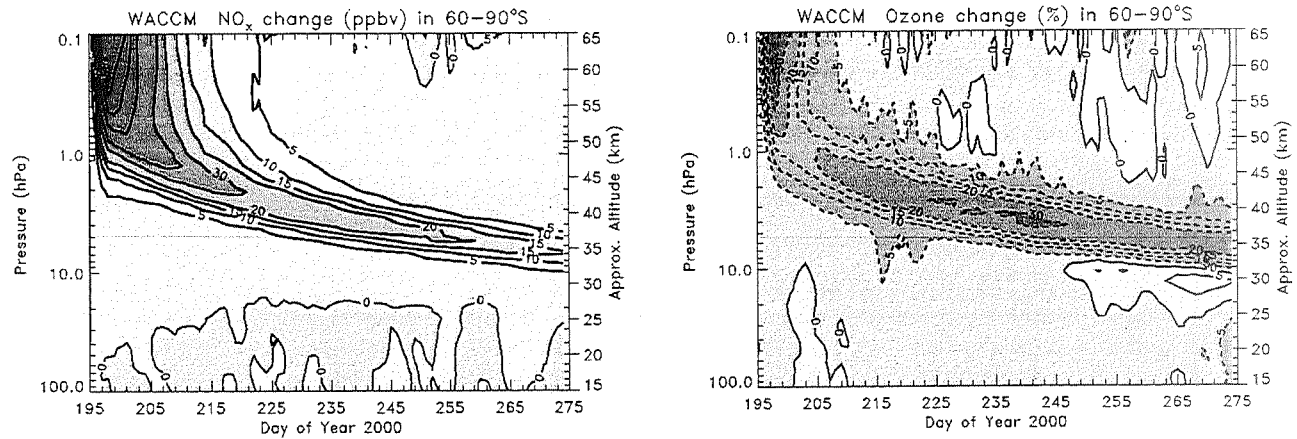


Figure 11. Derived from WACCM3 output showing the difference of the ensemble average of simulations 3(a,b,c,d) compared to the ensemble average of simulations 3(w,x,y,z) for the latitude band 60-90°S from day 195 (July 13) through day 275 (October 1) for year 2000. Left plot indicates NO<sub>x</sub> change with contour levels of 0, 5, 10, 15, 20, 30, 40, 60, 80, and 100 ppbv. Right plot indicates ozone change with contour levels of -40, -30, -20, -15, -10, -5, 0, and 5%.

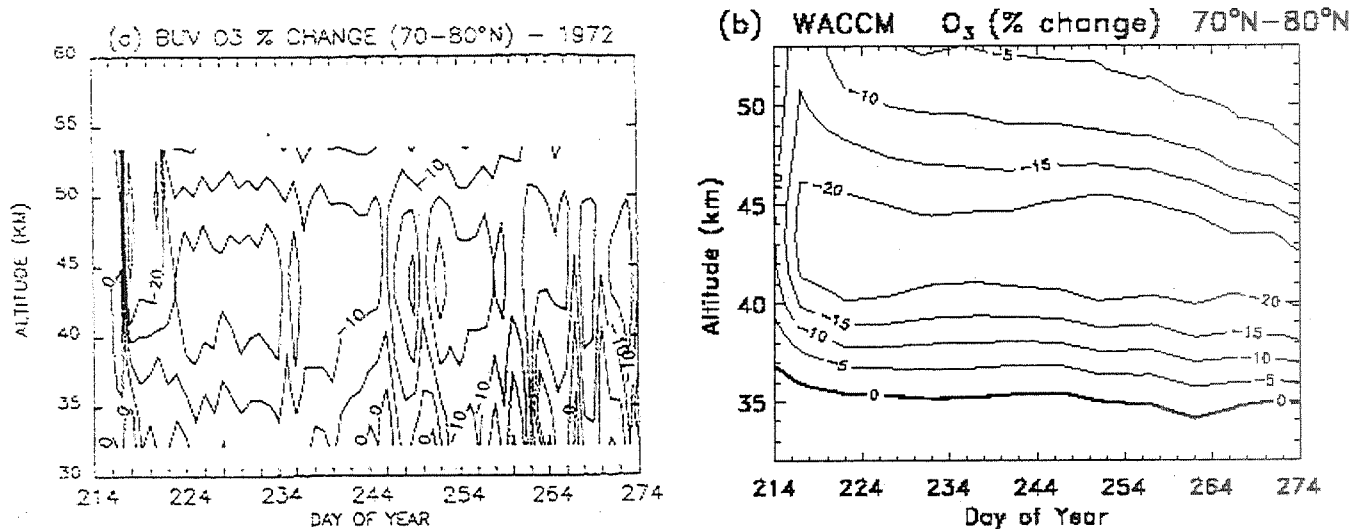


Figure 13. Plot (a) is taken from Figure 6 of Jackman et al. [1990] and shows the temporal evolution of measured ozone abundance changes in 1972 relative to 1970 by the backscattered ultraviolet (BUV) instrument aboard the Nimbus 4 satellite for the latitude band 70–80°N. Plot (b) is derived from the WACCM3 ensemble average of simulations 1(a,b,c,d) and indicates ozone changes in 1972 relative to 1970 in the same latitude bands. Contour levels plotted are -30, -20, -15, -10, -5, and 0%.

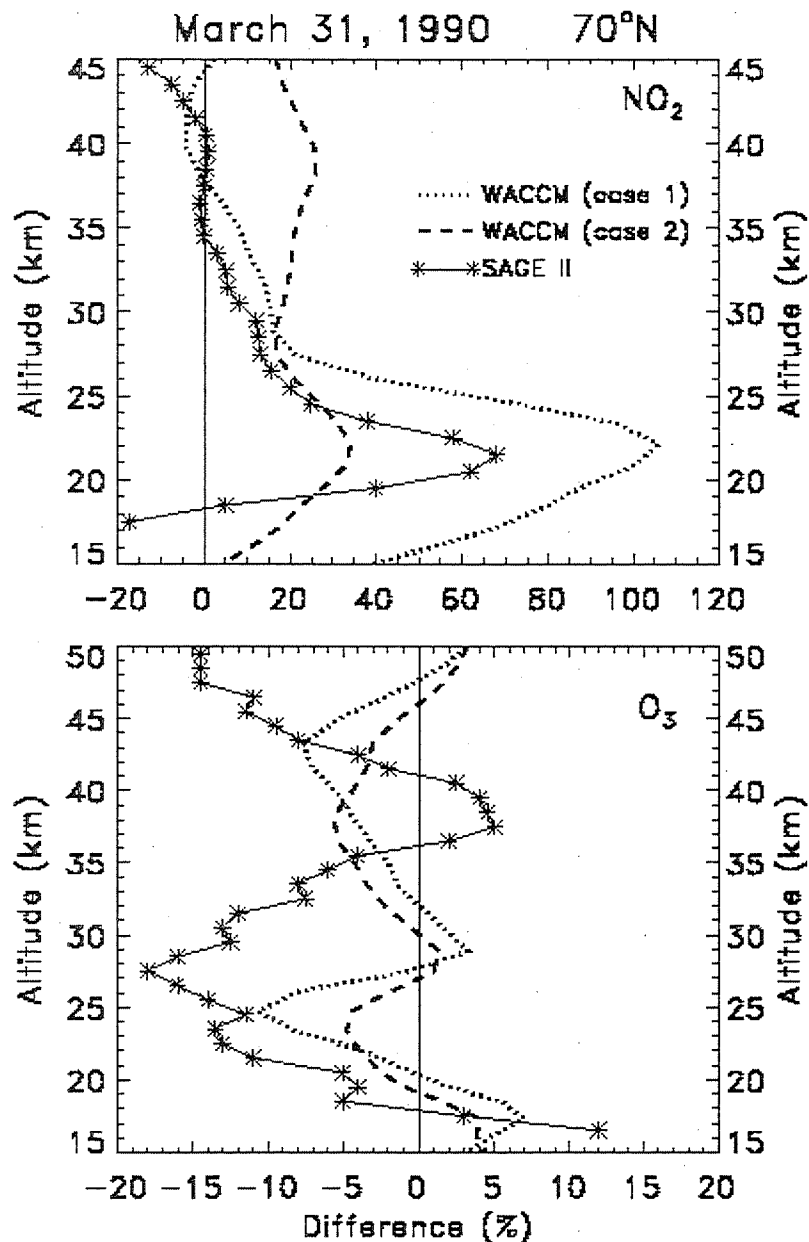


Figure 15. SAGE II measurements (solid line) and WACCM3 predictions (dashed and dotted lines) for  $70^\circ\text{N}$  zonal mean percentage change for March 31, 1990 for constituents (top)  $\text{NO}_2$  and (bottom)  $\text{O}_3$ . SAGE II results were derived by computing the percentage difference on March 31, 1990 compared with March 31, 1987. WACCM3 (case 1) was derived using the ensemble mean of simulations 1(a,b,c,d) and computing the percentage difference on March 31, 1990 compared with March 31, 1987. WACCM3 (case 2) was derived from the ensemble average of simulations 2(a,b,c,d) differenced with the ensemble average of simulations 2(w,x,y,z) for March 31, 1990.